

¹⁵C. Benoît à la Guillaume, F. Salvan, and M. Voos, *J. Luminescence* **1/2**, 315 (1970).

¹⁶It is noteworthy that one of the qualitative arguments used to distinguish between excitonic molecules and EHD is the kinetics of the new emission lines. In fact they are discrepancies between the results reported in Refs. 7 and 15, but in such experiments, one has to be very careful to the homogeneity of the excitation. In fact the problem of the kinetics in the EHD model is not yet fully resolved in our opinion.

¹⁷C. Benoît à la Guillaume and O. Parodi, in *Proceedings of the Fifth International Conference on Semiconductor Physics, Prague, 1960* (Academic, New York, 1961), p. 426.

¹⁸C. Benoît à la Guillaume, F. Salvan, and M. Voos, in Ref. 7, p. 516.

¹⁹C. Benoît à la Guillaume, M. Voos, and F. Salvan, *Phys. Rev. Letters* **27**, 1214 (1971).

²⁰We thank Dr. D. Adler for drawing our attention on that point.

²¹G. D. Pikus and G. L. Bir, *Fiz. Tverd. Tela* **1**, 1642 (1959) [*Sov. Phys. Solid State* **1**, 1502 (1960)].

²²I. Balslev, *Phys. Rev.* **143**, 636 (1966).

²³V. S. Bagaev, T. I. Galkina, and O. V. Gogolin,

in Ref. 7, p. 500.

²⁴J. C. Hensel and G. Feher, *Phys. Rev.* **129**, 1041 (1963).

²⁵Y. E. Pokrovskii and I. I. Svistunova, *Fiz. Tekhn. Poluprov.* **4**, 491 (1970) [*Sov. Phys. Semicond.* **4**, 409 (1970)].

²⁶J. D. Cuthbert, *Phys. Rev. B* **1**, 1552 (1970).

²⁷K. L. Shaklee and R. E. Nahory, *Phys. Rev. Letters* **24**, 942 (1970).

²⁸In the case of Si we have also used unpublished results of P. Nozières and M. Combescot to obtain the exact value of the mean exchange energies. They have shown that $\langle E_{ex}^e \rangle$ is reduced by a factor 0.94 and $\langle E_{ex}^h \rangle$ by a factor 0.88 when the anisotropy of the conduction band and the degeneracy of the valence band are taken into account.

²⁹B. W. Levinger and D. R. Frankl, *J. Phys. Chem. Solids* **20**, 281 (1961).

³⁰J. C. Hensel and K. Suzuki, in Ref. 7, p. 541.

³¹R. A. Faulkner, *Phys. Rev.* **184**, 713 (1969).

³²J. C. Hensel, H. Hasegawa and M. Nakayama, *Phys. Rev.* **138**, A225 (1965).

³³N. O. Lipari and A. Baldereschi [*Phys. Rev. B* **3**, 2497 (1971)] referred to unpublished results of P. Lawaetz.

Absorption and Electroabsorption of Trigonal Selenium near the Fundamental Absorption Edge

R. Fischer*

Physikalisches Institut der Universität Frankfurt/Main, Germany

(Received 27 May 1971)

The absorption spectrum and the spectrum of electroabsorption of vapor-grown trigonal Se platelets have been measured at various temperatures down to 2°K. The absorption curves for both $\vec{E} \parallel c$ and $\vec{E} \perp c$ show several steps at the onset of the absorption edge. No Urbach tail has been found. The steps are interpreted as arising from the indirect excitation of an exciton at 1.853 eV (low-temperature value) with several phonons. The electroabsorption spectra confirm the step structure within the absorption edge. Finally, it is shown that the luminescence of Se can also be explained with the same model.

I. INTRODUCTION

The band gap of trigonal selenium lies in the red part of the visible spectrum, at about 2 eV. This follows from optical properties of selenium single crystals.^{1,2} In spite of this advantage of an easy spectroscopy, great difficulties existed in measuring directly, i.e., by absorption measurements, whether the optical gap is direct or indirect. These difficulties arose mainly from the preparation of suitable single crystals: During these investigations both the absorption coefficient and the luminescence were found to be highly sensitive to pressure and deformation. Therefore no polishing may be applied to cleaved melt-grown crystals. On the other hand, vapor-grown crystals, which can be taken as-grown, were too thin to show fine structure

in the absorption edge at low absorption coefficients.³

Former band-structure calculations⁴ show the minimum band gap of selenium to be direct, but they do not exclude the alternative possibility, since the calculated bands are very flat in k space. Thus, small corrections would yield just the opposite result.

The most recent calculations⁵ give an indirect minimum band gap, though, of course, because of the flat bands, with the same restrictions.

Many spectroscopic methods have been applied to selenium in order to answer the question about the nature of the optical band gap. Absorption^{3,6} and reflection⁷⁻¹⁰ spectra and electroabsorption¹¹ and electroreflection¹² spectra have been experimentally studied. The absorption spectrum at He temperatures⁹ has been taken only from melt-grown

crystals. The spectrum with the \vec{E} vector of the incident light perpendicular to the crystal c axis has been interpreted as an Urbach tail¹³ of an excitonic absorption. For $\vec{E} \parallel c$ the spectrum is attributed to indirect transitions. Either edge is found to be shifted to lower energy with higher temperature.

Here the absorption spectra of relatively thick single-crystalline selenium platelets are reported. The measurements have been performed at and above He temperature. Both great thickness (approximately 300 μ) and low temperature allowed us to find a steplike structure which can easily be explained by indirect excitation of an exciton with the assistance of several phonons, and also by impurity-induced transitions. For a unique decision between these two interpretations, the temperature dependence of the absorption edge has been investigated. The results favor the model of the indirect excitonic transitions.

Additionally, electroabsorption data which confirm the distinct step structure found in the absorption edge are reported. It is shown, finally, that the "indirect" model also explains the well-known luminescence spectrum^{14,15} of trigonal selenium.

II. EXPERIMENTAL

A. Crystals

The trigonal crystals were grown from the vapor phase in the usual manner.¹⁶ Most of the crystals were in the shape of hexagonal hollow needles and, therefore, could not be taken for absorption measurements. The selenium melt, thus, was doped with TlCl to favor the growth of usable platelets.¹⁷ Se platelets of different origin¹⁸ also were investigated; they had been grown without doping the Se melt with TlCl, but yielded the same absorption spectra and the same luminescence. One can, therefore, conclude that doping of the melt does not influence the doping of the crystals.

Platelets which have been grown in this way are 10–500 μ thick. They possess two parallel surfaces or are slightly wedge shaped. The crystallographic c axis always lies in a surface plane and, in the case of wedge-shaped crystals, is perpendicular to the gradient of crystal thickness.

The surfaces look plane and smooth, even under the microscope, and additional preparation would only have damaged the crystals. The thickness variation of wedge-shaped crystals is always negligible since the monochromator slit is adjusted, in width and location, to an area where the thickness is essentially constant.

Before the measurement, the samples are cautiously clamped to the sample holder at one end to produce no strain. A reliable, though only

qualitative, indication for the presence of strain is the luminescence of the crystals. Luminescence is quenched close to the spot where the sample is clamped,¹⁴ and no luminescence is found from polished crystals.¹⁹

B. Absorption Spectra, Measurement, and Evaluation

The samples were illuminated with the full spectrum of an iodine tungsten lamp. The incident light was polarized and chopped in front of the cryostat, the chopping frequency being approximately 1 kHz. The transmitted light was analyzed by a double-grating monochromator and was detected by a photomultiplier and subsequent lock-in amplifier. The resolution of the monochromator was, with open slits, 8 Å corresponding to 2.3 meV in the region of interest. The selenium crystals were attached to a copper block and directly immersed into liquid He, H₂, or N₂. Intermediate temperatures could be attained by slowly warming up the copper block after the cooling liquid had been completely evaporated. The speed of warming up was small but finite. Therefore all these temperatures are affected by an error of about $\pm 2^\circ$ K. The temperature was measured using a calibrated carbon resistor on the copper block.

Some of the spectra were taken with monochromator and cryostat interchanged; the samples were thus illuminated with monochromatic light. The spectra did not change and therefore the more convenient setup as described above could be retained for all further measurements.

The formula

$$I/I_0 = (1 - R)^2 e^{-\alpha d} / (1 - R^2 e^{-2\alpha d}) \quad (1)$$

was applied for evaluation of the transmission spectra. I_0 and I are the intensity of incident and transmitted light, respectively, R is the reflection coefficient, α is the absorption coefficient, and d is the crystal thickness. The evaluation was simplified by the following assumptions:

(i) The denominator in Eq. (1) was set equal to unity. This is permissible for large αd . The relative deviation from the accurate value of α is in this case ($R = 0.25$ to 0.40) less than 1% if αd is larger than 1.4. The structure in the absorption spectra of all used crystals lies beyond this limit.

(ii) The reflection coefficient as a function of wavelength was taken from the literature.⁸ The factor $(1 - R)^2$ does not, however, affect the structure of the absorption edge.

(iii) For all crystals there was an extinction background due to scattering which varied from sample to sample but was constant over wavelength. This background was subtracted before evaluation.

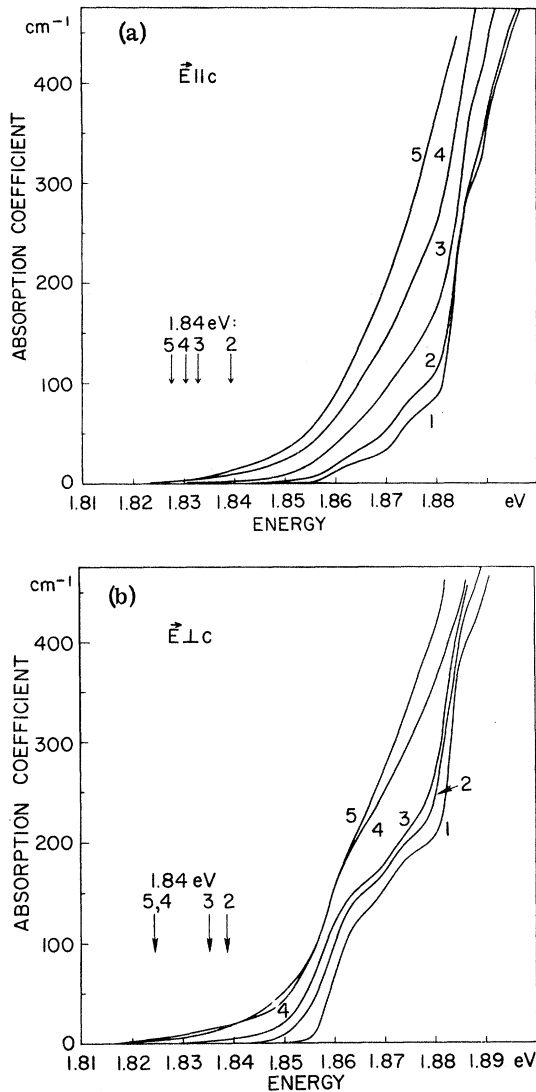


FIG. 1. Absorption spectra of a 220- μ -thick Se crystal at five different temperatures. The given energy scale is valid only for curve 1, 4.2°K, the other curves being shifted to lower energy. The arrows indicate 1.84 eV for the respective curves. (a) $\vec{E} \parallel c$, curve 1: 4.2°K, no shift; 2: 25.5°K, shifted by 0.6 meV; 3: 57.5°K, shifted by 7.2 meV; 4: 90.0°K, shifted by 9.5 meV; 5: 122.0°K, shifted by 12.3 meV. (b) $\vec{E} \perp c$, curve 1: 4.2°K, no shift; 2: 30.0°K, shifted by 1.4 meV; 3: 65.0°K, shifted by 4.8 meV; 4: 93.0°K, shifted by 15.7 meV; 5: 121.0°K, shifted by 15.7 meV.

C. Electroabsorption

For the measurement of the electroabsorption a coplanar structure was used: The platelet-shaped crystals received gold contacts on one side, the spacing between the electrodes being 1 mm. The contacts were evaporated in vacuum better than 10^{-4} Torr. Only the region halfway between

the contacts was focused on the monochromator slit, since only there was the electric field very homogeneous. Electric field \vec{E} , propagation vector \vec{k} of the incident light, and crystal c axis were perpendicular to each other.

The absorption setup could be kept as described above with some variations. These variations were suggested by the difficulty of transferring heat away from the sample, since in the used structure the applied electric field always produces a current. (1) The coolant was liquid He below the λ point, since superfluid He is an extremely good heat conductor. (2) The samples were illuminated only through the monochromator and not with the full lamp spectrum in order to minimize photoconductivity and joule heat production. Applying these precautions, a maximum field of 10^4 V/cm could be attained.

In the case of electroabsorption the reference signal was generated by the lock-in amplifier. An ac voltage (at the reference frequency) was used to trigger an electronic switch on the dc high-voltage supply. The voltage pulses had a repetition frequency of 20–200 Hz. In this range the signal did not depend on frequency. The signal was always in phase with the applied voltage.

III. RESULTS

A. Absorption

Figures 1(a) and 1(b) show the absorption curves of trigonal Se for $\vec{E} \parallel c$ and $\vec{E} \perp c$ at various temperatures. The spectra of both figures have been taken from the same 220- μ -thick crystal.

$\vec{E} \parallel c$, Fig. 1(a): Four steps can distinctly be seen in curve 1: Two of about equal size at 1.859 and 1.872 eV, a very steep one at 1.883 eV, and the fourth at 1.890 eV. We tried to find these steps, at least the three first ones, in the absorption spectra at higher temperatures, without regard to their heights and their absolute position on the energy axis. Curves 2 and 3 still show the two first steps clearly; in spectra 4 and 5, however, this structure can only be determined approximately. In Fig. 1(a) the spectra at different temperatures are plotted to show the closely related structures rather than the absolute energy value. The arrows labeled with the respective curve numbers indicate the shift of the energy scale.

$\vec{E} \perp c$, Fig. 1(b): These spectra are very similar to those with $\vec{E} \parallel c$, except that the height of the first step at 1.859 eV is distinctly larger. The curves at different temperatures also were plotted with different energy scales to show their relationship in structure. Note that both temperatures and shifts are different from the spectra of Fig. 1(a). The shift of the absorption edge of trigonal selenium can be obtained from the shift of the en-

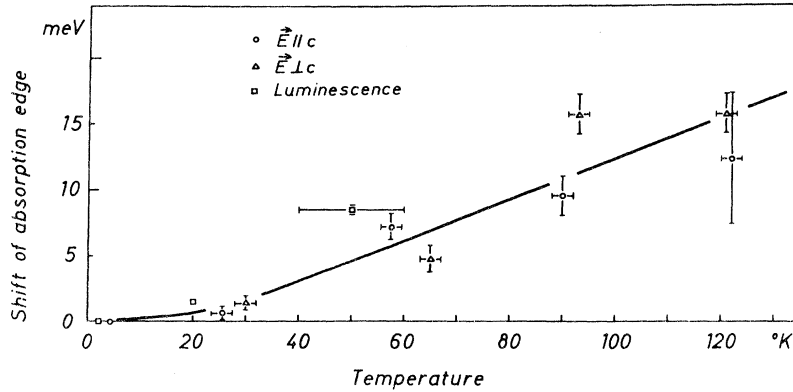


FIG. 2. Shift of the absorption edge of Se with temperature for both $\vec{E} \parallel c$ and $\vec{E} \perp c$. The diagram also contains the energy shift of the luminescence lines (Refs. 14 and 19).

ergy scales in Figs. 1(a) and 1(b) and is plotted in Fig. 2. This diagram also contains the energy shift of the luminescence lines of selenium. The slope of this curve, i. e., the differential absorption-edge shift, is zero at 0 °K and yields $+(1.6 \pm 0.5) \times 10^{-4}$ eV/deg near 100 °K. This value is different from the result obtained from isoabsorption curves, which yield a negative temperature coefficient.⁶

B. Electroabsorption

Figures 3(a) and 3(b) contain the electroabsorption spectra of selenium for $\vec{E} \parallel c$ and $\vec{E} \perp c$ at about 1.8 °K. The spectra were taken from a 293- μ -thick platelet. Both figures also show the absorption curves at 4.2 °K in order to demonstrate the close relationship between absorption and electroabsorption. The difference in temperature (1.8 vs 4.2 °K) is not important since the absorption edge does not shift (Fig. 2) and since there is practically no change in the phonon Bose factor. The curves were measured with 20-Hz repetition frequency of the voltage pulses with an electric field of 5×10^3 V/cm in the sample. Additional structure did not show up at lower fields.

For $\vec{E} \parallel c$ [Fig. 3(a)] one can see mainly three lines at the energies 1.858, 1.872, and 1.883 eV. The third line reaches about ten times the height of the two first lines. The comparison with the absorption spectrum shows that the main maxima of the electric effect are always located at the beginning of a step in the absorption curve. The heights of the maxima reflect well the steepness of the respective steps in absorption. Therefore a further maximum at 1.89 eV is postulated, though not found because of the low transmission at this energy.

The $\vec{E} \perp c$ spectrum looks very much like the $\vec{E} \parallel c$ spectrum except for the higher first maximum, in accurate correspondence to the steeper first step in the absorption spectrum for $\vec{E} \perp c$. The field dependence has been measured for the three

main lines with $\vec{E} \parallel c$ and for the line at 1.858 eV with $\vec{E} \perp c$. In all cases the electroabsorption goes as the square of the electric field and the plots are very similar. Consequently, only one example is given in Fig. 4 ($\vec{E} \parallel c$, 1.858 eV). The saturation at high fields is most probably due to heating of the crystal.

IV. DISCUSSION

A. Absorption

The steps or edges in the absorption spectra can be interpreted by the indirect excitation of an exciton^{20,21} or by band-to-band transitions with ionization of impurities.²¹ One means of distinguishing between these two explanations is the temperature dependence of the absorption coefficient.

(i) Impurity-to-band transitions should not depend on temperature in a rough approximation. This can be seen by considering transitions, e. g., from a filled valence band to empty donor states. If the donor states are sufficiently localized, they have a large extension in \vec{k} space. Therefore vertical transitions from the valence band to the donors are allowed not only for $\vec{k}=0$ but also for $\vec{k} \neq 0$. This yields an absorption edge $\alpha(E)$ which is proportional to $(E - E_0)^{1/2}$, E_0 being the distance from the maximum of the valence band to the donor level. The square-root dependence of α on energy produces a step in the absorption spectrum, but in this approximation no temperature dependence of the absorption coefficient is induced.

(ii) Phonon-assisted transitions to indirect exciton levels also yield steps in the absorption edge.²⁰ They are, however, very temperature sensitive through the Bose factors $B(\hbar\omega, T) = 1/(e^{\hbar\omega/kT} - 1)$, $\hbar\omega$ being the energy of the phonon.

Since the measured spectrum—at least for $\vec{E} \parallel c$ —depends strongly on temperature, and since excitons are found to be of great influence²² in Se, we attempt now to fit to the results the theoretical expressions for phonon-assisted transitions to

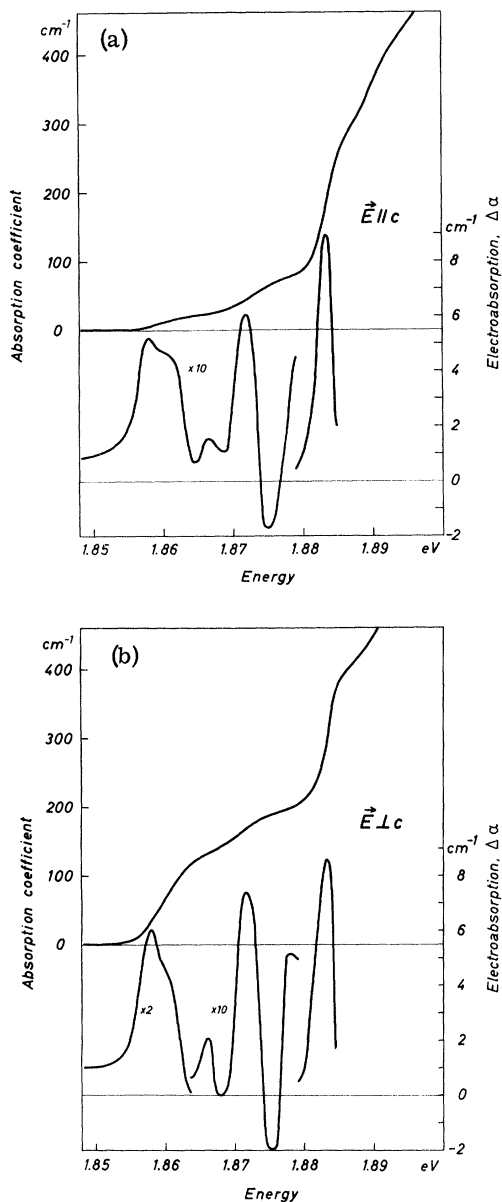


FIG. 3. Spectra of the electroabsorption $\Delta\alpha$ at 1.8°K, electric field: 5×10^3 V/cm. For comparison the absorption spectra at 4.2°K are plotted over the same energy scale: (a) $\vec{E} \parallel c$; (b) $\vec{E} \perp c$.

indirect excitons. For several phonon branches (number n) the following expression is given by theory²³:

$$\alpha(h\nu, T) = \sum_{i=1}^n A_i \{ (h\nu - E_0 - \hbar\omega_i)^{1/2} [1 + B(\hbar\omega_i, T)] + (h\nu - E_0 + \hbar\omega_i)^{1/2} B(\hbar\omega_i, T) \}. \quad (2)$$

This formula accounts for emission and absorption of phonons. The constants A_i include the phonon matrix elements, the mass of the exciton with re-

spect to translation ($m_h^* + m_e^*$), and the derivative of the hydrogen envelope function of the exciton. E_0 is the (thermal) excitation energy of the indirect exciton.

The A_i contain more detailed information about the exciton than is within the scope of these investigations. They are therefore treated as fitting parameters. The ω_i can be taken from ir absorption, Raman effect, and neutron scattering. One has to remember, however, that ir absorption, Raman effect, neutron scattering, and indirect absorption yield the phonon energies at different wave vectors. Therefore minor corrections in the ω_i are permitted in order to obtain a uniquely defined E_0 .

The first three steps in Fig. 1 can be ascribed to the three phonon branches²⁴ of selenium. Table I contains the data for the best fit of Eq. (2), $n = 3$, to the spectrum of $\vec{E} \parallel c$ at 4.2°K (treated as 0°K). The corresponding theoretical and experimental curves are shown in Fig. 5(a). The characteristic energies for the absorption steps and the A_i were determined by plotting $\alpha(E)$ as α^2 vs E , obtaining a straight line for the first edge. A_1 and $\hbar\omega_1$ were taken, respectively, from the slope of that straight line and its intersection with the

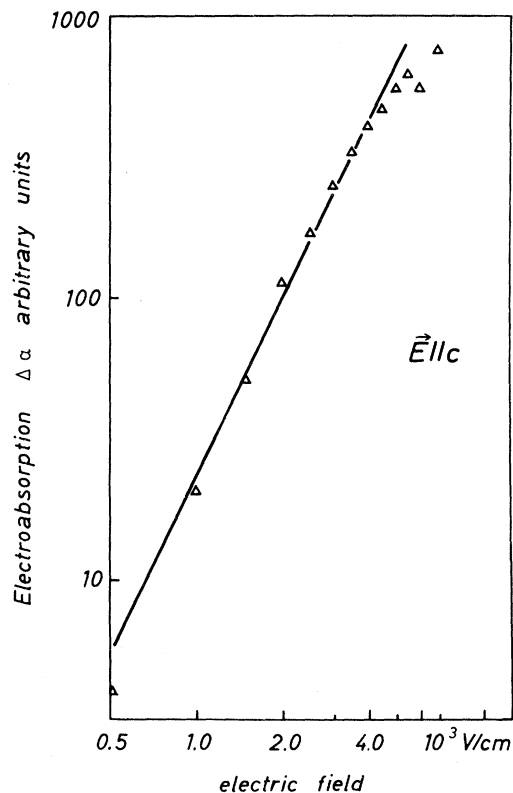


FIG. 4. Field dependence of the electroabsorption for $\vec{E} \parallel c$, at the energy of 1.883 eV (low-energy maximum).

TABLE I. Data for the best fit of Eq. (2) to the absorption curve for $\vec{E} \parallel c$, 4.2 °K.

Characteristic energy (eV)	Absorption process	Phonon branch and method for determining its energy	Parameters A_i ($\text{cm}^{-1} \text{eV}^{-1/2}$)
1.853	$E_0 =$ indirect exciton level		
1.859	$\hbar\nu = E_0 + \hbar\omega$ $\hbar\omega_1 = 5.1 \text{ meV}$	acoustic branch, neutron diffraction ^a	275.1
1.872	$\hbar\nu = E_0 + \hbar\omega_2$ $\hbar\omega_2 = 18.1 \text{ meV}$	first optical branch, ir absorption, ^b Raman scattering, ^c neutron diffraction ^a	468.0
1.883	$\hbar\nu = E_0 + \hbar\omega_3$ $\hbar\omega_3 = 29.3 \text{ meV}$	second optical branch, ir absorption, ^b Raman scattering, ^c neutron diffraction ^a	3040.0

^aReference 28.^bReference 24.^cG. Lucovsky, R. C. Keezer, and E. Burstein, Solid State Commun. 5, 439 (1967).

energy axis. With these values for A_1 and $\hbar\omega_1$ the first edge was subtracted from the whole absorption edge. A_2 , $\hbar\omega_2$ and A_3 , $\hbar\omega_3$ could be obtained by repeating this procedure. The fourth step at 1.890 eV cannot be included since selenium possesses only three phonon branches.

After this fit the spectra for $\vec{E} \parallel c$ at higher temperatures were calculated. As an example, the calculated and measured spectra at 90.0 °K are shown in Fig. 5(b). The coincidence in details is not very good, but the over-all shape is satisfactorily reproduced. This discrepancy in details is explained as follows: (1) Phonon branches, in general, are not horizontal, but the theoretical expression [Eq. (2)] assumes that they are. (2) At high temperatures, exciton levels tend to be thermally broadened,^{21,25} but the theory only deals with sharp levels.

Such a good over-all fit could only be obtained for $\vec{E} \parallel c$. It can be seen from Fig. 1(b) that the first step with $\vec{E} \perp c$ exhibits a much weaker temperature dependence than the other edges and the edges for $\vec{E} \parallel c$ do. This by itself leads to the following explanation: The absorption spectrum for $\vec{E} \perp c$ is the superposition of a spectrum like $\vec{E} \parallel c$ and a spectrum which is almost temperature independent and, therefore, cannot be interpreted in the same way as the spectrum for $\vec{E} \parallel c$.

It is tempting to consider the results of this discussion in the framework of band-structure calculations. No selection rules for indirect transitions are available until now and that is why Table II deals only with energy separations between valence-band maxima and conduction-band minima. The energy values are taken from pseudopotential calculations.⁵ Their results suggest a minimum in-

direct band gap from M to A , thus predicting the experimental value to within $\pm 50\%$ (the experimental value for E_0 has still to be enlarged by the exciton binding energy).

B. Electroabsorption

The results of the electroabsorption measurements are given in this context to confirm the structure in the absorption edge. The electroabsorption spectra clearly arise from transitions to an indirect exciton involving the emission of phonons. Spectra corresponding to phonon absorption could not be detected at higher temperatures. This is due to the fact that the absorption edge loses much of its structure at temperatures higher than about 30 °K, where phonon absorption is still weak.

C. Absorption and Luminescence

In this section it will be shown that the luminescence of trigonal selenium^{14,19} fits well into the model which has been developed for the interpretation of the absorption results. Furthermore, the

TABLE II. Energy separations.

Valence band	Conduction band	Location of band extrema in Brillouin zone ^a	Location of required phonon in Brillouin zone	Calculated energy distance ^a (eV)
M	\rightarrow	A	L	1.3
M	\rightarrow	H	axis $\Gamma-K'$	1.6
H	\rightarrow	A	K	1.8
Γ	\rightarrow	H	A	1.8
M	\rightarrow	M	(direct transition)	1.9

^aReference 5.

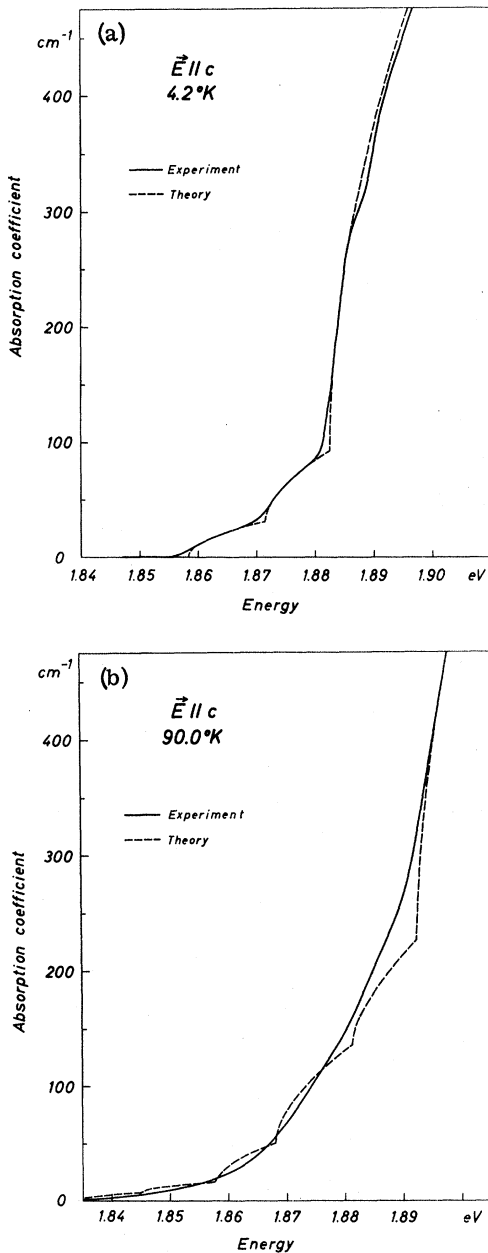


FIG. 5. (a) Fit of the theoretical expression for phonon-assisted excitonic absorption to the absorption spectrum $\vec{E} \parallel c$ at 4.2°K . (b) Absorption spectrum $\vec{E} \parallel c$, calculated after the fit for 90.0°K (dashed line) and the corresponding experimental curve (solid line).

model gives also a satisfactory explanation for the temperature dependence¹⁴ of the luminescence and for the behavior of the luminescence lines in an electric field.¹⁹

The luminescence spectrum of selenium, at 4.2°K , consists of a series of seven lines in the energy range 1.81–1.85 eV (Fig. 6, left-hand

side) and phonon replicas of these lines at an energy lower by 29 meV.¹⁵

Each of these lines reacts differently on variation of temperature and on an electric field: Lines 2, 4, and 6 disappear both at temperatures above 4.2°K and in an electric field of sufficient strength. In both cases lines 0, 3, and 5 and, maybe, line 1 remain constant. How line 1 behaves could not be determined with certainty.¹⁹

In Fig. 6 the luminescence spectrum looks like the mirror image of the absorption edge, if one assumes that a steep absorption step corresponds to a strong luminescence line, a low step to a weak line, and so on. The mirror plane then lies at about 1.855 eV. This phenomenon is even more pronounced if one compares the spectra of electroabsorption—instead of the absorption edge—with the luminescence spectrum.

The luminescence can now be explained in the following manner: At low temperatures absorption of phonons is not possible; therefore both optical absorption and luminescence can only take place with emission of phonons. Thus the indirect excitation of a level at the energy E_0 requires an energy of $E_0 + \hbar\omega$ of the absorbed photon, $\hbar\omega$ being a phonon energy, whereas the decay of that excited state gives a photon energy of only $E_0 - \hbar\omega$.

This simple model explains lines 0, 3, and 5 of the luminescence, each of them corresponding to the decay of the indirect exciton at 1.853 eV with emission of phonons from the three phonon branches of Se.

One can explain lines 2, 4, and 6 if one assumes a shallow acceptor located 4.8 meV above the valence-band edge. This simply seems to be an *ad hoc* assumption, but there is nevertheless much evidence for shallow acceptors in selenium—first of all, the fact that Se is only found to be *p* type at low temperature.²⁶ These acceptors are neutral at 4.2°K and therefore cannot be detected in absorption. The temperature and electric field dependence of the luminescence lines 2, 4, and 6 are also explained by these low-binding-energy

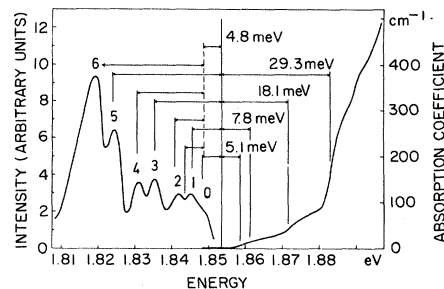


FIG. 6. Luminescence (Refs. 14 and 19) and absorption of trigonal Se, both at 4.2°K .

acceptors. That is, (i) at temperatures higher than 4.2 °K the acceptors become negative, and the corresponding lines disappear, and (ii) electric fields of about 10^4 V/cm are able to ionize these shallow impurities and thus can quench lines 2, 4, and 6—in complete agreement with experiment.¹⁹ Line 1 is most likely to come from the decay of the indirect exciton with a phonon at 7.8 meV. This phonon energy clearly belongs to the acoustic branch and is also associated with a maximum of phonon density of states, as follows from neutron diffraction.²⁷ The contribution of this phonon is not resolved in absorption but is distinctly resolved in electroabsorption [Figs. 3(a) and 3(b)]: The peak at 1.858 eV can be resolved into two lines, one at 1.858 and the other at 1.862 eV.

V. SUMMARY AND CONCLUSIONS

According to these results and their interpretation the absorption edge of trigonal selenium in the visible region is characterized as follows:

The lowest electronic energy level of selenium is an exciton level at 1.853 eV which can only be reached indirectly, with assistance of phonons. Thus the absorption edge looks very much like those in germanium,²⁸ silicon,²⁹ GaP,³⁰ and HgS.³¹ The indirect nature of the edge has been established by its temperature dependence for $\vec{E} \parallel c$ and, with restrictions, for $\vec{E} \perp c$.

Thus Se is an indirect semiconductor, its smallest gap being 1.853 eV plus the binding energy of that exciton. The binding energy has not yet been determined.

It is emphasized that no Urbach tail could be detected. The Urbach tail found previously is resolved into phonon steps in the absorption edge.

This model is successful, too, in explaining the luminescence of Se. With the assumption of an acceptor with a binding energy of 4.8 meV every line in the luminescence spectrum could be assigned to an indirect transition from the same exciton state.

The fourth step in the absorption edge at 1.890 eV, however, still lacks interpretation. It may be due to the onset of transitions to another indirect exciton. The different indirect gaps may be very close together in energy, since the energy bands of Se are very flat.⁵

ACKNOWLEDGMENTS

I would like to thank Professor H. Queisser very much for stimulation and encouragement, Professor J. Stuke and Dr. G. Weiser, University of Marburg, for their help in supplying some of the crystals, and all of them and my colleagues from the University of Frankfurt for many interesting discussions.

*Present address: Physikalisches Institut der Universität Marburg/Lahn, Germany.

¹J. Stuke, in *The Physics of Se and Te* (Pergamon, New York, 1969), p. 3.

²J. Stuke and H. Keller, *Phys. Status Solidi* **7**, 189 (1964).

³W. Henrion, *Phys. Status Solidi* **12**, K113 (1965).

⁴J. Treusch and R. Sandrock, *Phys. Status Solidi* **16**, 487 (1966).

⁵R. Sandrock, *Phys. Rev.* **169**, 642 (1968).

⁶G. G. Roberts, S. Tutihasi, and R. C. Keezer, *Phys. Rev.* **166**, 637 (1968).

⁷W. Henrion, *Phys. Status Solidi* **20**, K145 (1967); **22**, K33 (1967).

⁸S. Tutihasi and I. Chen, *Phys. Rev.* **158**, 623 (1967).

⁹S. Tutihasi and I. Chen, *Solid State Commun.* **5**, 255 (1967).

¹⁰E. Mohler, J. Stuke, and G. Zimmerer, *Phys. Status Solidi* **22**, K49 (1967).

¹¹J. Stuke and G. Weiser, *Phys. Status Solidi* **17**, 343 (1966).

¹²G. Weiser and J. Stuke, in *Proceedings of the International Conference on the Physics of Semiconductors*, edited by S. M. Ryvkin (Nauka, Leningrad, 1968), Vol. 1, p. 228.

¹³F. Urbach, *Phys. Rev.* **92**, 1324 (1953).

¹⁴H. Zetsche and R. Fischer, *J. Phys. Chem. Solids* **30**, 1425 (1969).

¹⁵H. Queisser and J. Stuke, *Solid State Commun.* **5**, 75 (1967).

¹⁶F. C. Brown, *Phys. Rev.* **4**, 85 (1914).

¹⁷R. Keezer, C. Wood, and J. W. Moody, in *Proceedings of the International Conference on Crystal Growth* (Pergamon, New York, 1967).

¹⁸The cooperation of Dr. G. Weiser, University of Marburg, Germany—he supplied these crystals—is thankfully acknowledged.

¹⁹K. H. Kühler (private communication).

²⁰For example, J. O. Dimmrock, in *Semiconductors and Semimetals*, edited by R. K. Willardson and A. C. Beer (Academic, New York, 1967), Vol. 3, p. 259.

²¹E. J. Johnson, *Ref.* **20**, p. 153.

²²R. Fischer, *Phys. Status Solidi* **31**, K139 (1969).

²³R. J. Elliott, *Phys. Rev.* **108**, 1384 (1957).

²⁴R. Geick, U. Schröder, and J. Stuke, *Phys. Status Solidi* **24**, 99 (1967).

²⁵M. D. Sturge, *Phys. Rev.* **127**, 768 (1962).

²⁶J. Stuke, *Festkörperprobleme* **5**, 111 (1966).

²⁷A. Axmann and W. Gissler, *Phys. Status Solidi* **19**, 721 (1967).

²⁸G. G. Macfarlane, T. P. McLean, I. E. Quarrington, and V. Roberts, *Phys. Rev.* **111**, 1245 (1958).

²⁹G. G. Macfarlane, T. P. McLean, I. E. Quarrington, and V. Roberts, *Phys. Rev.* **108**, 1377 (1957).

³⁰P. J. Dean and D. G. Thomas, *Phys. Rev.* **150**, 690 (1966).

³¹R. Zallen, in *II-VI Semiconducting Compounds*, edited by D. G. Thomas (Benjamin, New York, 1967), p. 877.